Counting of Uneaten Floating Feed Pellets in Water Surface Images using ACF Detector and Sobel Edge Operator

Conference Paper · October 2021

DOI: 10.1109/R10-HTC53172.2021.9641579

8 authors, including:

Maria Gemel B Palconit
Cebu Technological University
50 PUBLICATIONS **272** CITATIONS
SEE PROFILE

Ronnie Concepcion II
De La Salle University
249 PUBLICATIONS **1,498** CITATIONS
SEE PROFILE

Jonnel Alejandrino
De La Salle University
59 PUBLICATIONS **672** CITATIONS
SEE PROFILE

Ivan Roy Santiago Evangelista
Sultan Kudarat State University
9 PUBLICATIONS **18** CITATIONS
SEE PROFILE

Counting of Uneaten Floating Feed Pellets in Water Surface Images using ACF Detector and Sobel Edge Operator

Maria Gemel B. Palconit*[1], Ronnie S. Conception II[1], Jonnel D. Alejandrino[1], Ivan Roy S. Evangelista[3],
Edwin Sybingco[1], Ryan Rhay P. Vicerra[2], Argel A. Bandala[1], Elmer P. Dadios[2]
[1]*Electronics and Communications Engineering, De La Salle University, Manila, Philippines*
[2]*Manufacturing and Management Engineering, De La Salle University, Manila, Philippines*
[3]*Electronics Engineering, Sultan Kudarat State University, Philippines*
{*maria_gemel_palconit, ronnie_concepcionii, jonnel_alejandrino,
edwin.sybingco, ryan.vicerra, argel.bandala, elmer.dadios}@dlsu.edu.ph; ivanroyevangelista@sksu.edu.ph

***Abstract*—Determination of excess feed pellet count is an essential indication of fish feeding behavior responses. To date, computer vision (CV) is considered the most practical technique to detect and count the leftover pellets. It is primarily economically viable, has broad application to other fields, and has rapid advances in computing algorithms such as deep learning (DL). This study introduces a hybrid of aggregated channel feature (ACF) detector, a non-DL object detector, and Sobel edge operator, a basic CV algorithm, to detect and count the excess floating feed pellets in water surface images with varying background noises. The ACF was used to detect the region proposal (RP) candidates of leftover pellets and discriminate the RP with low confidence scores. The selected RPs for a group of pellets, i.e., greater than 400 pixels, were further processed using the Sobel edge operator to count each pellet in the RPs. In contrast, the RPs with a pixel size of 400 are considered as a single pellet. Then, all the counted pellets in each RPs were added. This approach resulted in a considerable pellet counting estimator with r^2 of 0.8 and NRMSE of 11.55% with a selected confidence score greater than 60. The main advantage of the proposed technique is that it only requires a substantially lower computational cost than a DL-based object detector.**

Keywords—Excess feed counter, computer vision, ACF Detector, Sobel Edge Operator

I. INTRODUCTION

Fish feed meal accounts for 65% to 70% of production expenses in aquaculture [1]. The leftover feed meal denotes economic loss and accelerates water pollution. Based on the study of [2], uneaten pellets can occur for as high as 50% of the distributed feeds. In essence, proper feeding management and control by monitoring the feed waste are necessary to obtain an efficient feeding system [2] [3]. Several approaches detected the excess feed pellets, such as acoustic beam, echo sounders, infrared sensors, and computer vision, among others [3]–[5]. Broadly, it is worth noting that computer vision (CV) has substantial growth in object detection and recognition in many areas in agriculture, such as plant phenotyping and fish detection [6]–[9]. In the context of the non-invasiveness, ease of development, flexibility to different applications (including excess feed detection), and economical solution, the CV is advantageous over other present technologies [5].

Specifically, the monitoring of feed waste is used as an indirect indication of fish feeding behavior responses wherein the detected feed waste is utilized as an interactive feedback mechanism to limit or adjust the amount of feed distribution. The monitoring and feedback of detected count of excess feed in real-time and remote manner can be obtained using the Internet of Things such as the studies of [10]–[17]. At the same time, the CV algorithm of the excess feed detection can be fused with a deep learning algorithm for higher accuracy [3][5]. Since 2015, there are only three published studies for excess feed detection in underwater images. The studies of [3] and [18] have used similar platforms for data acquisition wherein pellets are placed in a fixed white plate. The results showed a true positive detection for about 80% to 95.9% in a non-uniform illumination using different thresholding algorithms such as adaptive thresholding, multi-threshold Otsu, 2-D entropic, and Gaussian mixture model (GMM) coupled with adaptive thresholding with a maximum computing time of 235 seconds. Considering the real-time detection and detection accuracy on various background noises scenarios such as blurred images, random objects on the background, occlusion, minuscule target, and different feed density, the study of [5] using deep learning (DL) algorithm—You Only Look Once-version 4 (YOLO-V4) obtained a superior result over the study of [18] with a maximum detection accuracy of 92.61%.

Between the two detection methods, the traditional CV is often preferred for low-cost microcontroller because of its transparency, deployment versatility in computing devices due to low computational cost, and power efficiency. The traditional CV can be as simple as color thresholding and segmentation, linear filtering, and edge detection. The algorithms like Scale Invariant Feature Transform (SIFT) and Speeded Up Robust Features (SURF), among others, are deemed more sophisticated CV methods for object detection in which the feature variable is manually extracted and selected to develop a classifier with shallow structures. Conversely, the DL, a subset of machine learning (ML), learns both the feature descriptor and classifier; thus, its network structure is enormous. Although the object detection using DL is more accurate than the traditional CV methods, the major drawbacks of the former are generally the time spent for manual annotation and training, a large number of high-quality datasets needed for training, the requirement of large storage hardware, high-powered processors, and computing resources. Moreover, the transparency of the networks developed in DL is difficult to interpret due to the non-linear interaction between many network nodes and parameters; thus, there is often a black-box relationship between the input and the corresponding decision or output. In the context of overcoming the challenges between the two approaches, the hybrid models between CV and DL are deemed to have a satisfactory detection accuracy with lesser preparation time and computing requirements needed for implementation[19] [20].

This paper uses a combination of aggregated channel feature (ACF) and Sobel edge operator to detect the excess feeds. The ACF is a type of machine learning object detector.

978-1-6654-3240-5/21/$31.00 ©2021 IEEE

Compared to DL, the training time is faster and requires lesser annotated objects for training. In most studies, the ACF is utilized before the DL algorithm to quickly determine the region proposal candidates and improve the detection accuracy of existing DL algorithms such as YOLO and Faster R-CNN[21][22].

Alternatively, this paper utilizes the ACF to generate the region of interest (ROI) of the detected feeds along with the Sobel edge operator to count the group of feed pellets by detecting the edges of each pellet instead of DL. The Sobel edge operator is widely used to detect the edges of the objects in images due to its simplicity, low computational cost, and sensitivity to noises [23]. With the proposed approach, the number of input images and annotated objects used for training and the training time is significantly reduced compared to DL-based or a combination of ACF and DL detection methods. Another advantage of the proposed method over the DL is that it can quickly facilitate images for training with several labeled pellets per image, for which, when the same training dataset is run in DL platform will exceed to maximum allowable memory size due to the limitation of the GPU even with minimal layer network is selected, hence requires further image pre-processing by either tiling or resizing the images. Unfortunately, since the feed pellets are small, mere resizing the images for training is not a good option; thus, tiling requires stitching during post-processing.

Considering the type of pellets, this paper intends to detect the extruded floating pellets on the water surface as opposed to the studies of [3] [5][18], which detect the excess sinking pellets in underwater images. While different fish have different preferences of pellet type as such for halibut, which revealed to have better feeding responses to sinking pellets [24], the studies of [25][26] suggested that the floating pellets can obtain the best growth and economic performance for juvenile olive flounder and Nile tilapia. Another advantage for floating pellets in an automated excess pellet detection system using computer vision is that there is no need to submerge the camera, thus cheaper, and requires lesser cleaning maintenance than the latter due to the adherence of algae on the camera case. Generally, this study aims to detect and count the excess floating feed pellets in water surface images using the ACF detector and Sobel edge operator with non-uniform background noises such as different illumination, presence of fish, water bubbles, and reflection in water surfaces. The motivation of this approach is to provide another technique for object detection with less computation cost and usage of fewer input images for training compared to DL.

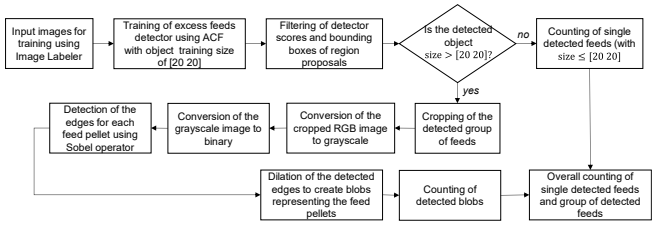

Fig. 1: Workflow of the Proposed Excess Feed Pellet Detector

II. Methodology

The workflow of the excess feed pellet counter is depicted in Fig. 1, which describes the processes from the input images, training of excess feed ROI detection, filtering of scores in suggested ROIs, excess feed detection using the Sobel edge operator, and counting of all the detected feeds. All processes are executed in MATLAB 2019b using Intel Core i7-8850U CPU at 1.8GHz (8 CPUs) with a memory of 16GB RAM and NVIDIA GeForce MX150 graphics processing unit.

A. Input Images and Training

There are ten input images with 720×1280 pixel resolution at 96 dpi. The images were annotated using the Image Labeler app—a toolbox in MATLAB 2019b used to label excess feed ROIs. The leftover feed pellets, whether a single pellet or a group of pellets, are all labeled (with bounding boxes) as 'feed' and are subjected to different background conditions such as reflective water surfaces, water bubbles, random presence of fish, uneven illumination, and color intensity as depicted in Fig. 2a while the count of labeled ROIs for the pellets per image is shown in Fig. 2b. The annotated images served as a ground truth, then fed to the ACF object training detector with an object training size of 20×20 pixels.

B. Confidence Scores of the Region Proposals

After training the ten images, the performance of the trained feed pellet ACF detector was checked using 20 images. In here, each region proposal (RP) of possible detected feed candidate has a corresponding confidence score, S. To filter out the weak RP candidates, they were filtered out such that the considered RPs were tested with the following confidence scores of $S > S_s$ where S_s are the confidence scores with the following testing values of $S_s = \{60, 70, 80, 90, 100\}$.

C. Detection and Counting of Feed Pellets

1) Detection of Single Feed Pellet

The detected RP with a bounding box sizes of 20×20 is considered as a single pellet. In this condition, all detected single pellets, P_s, were directly added.

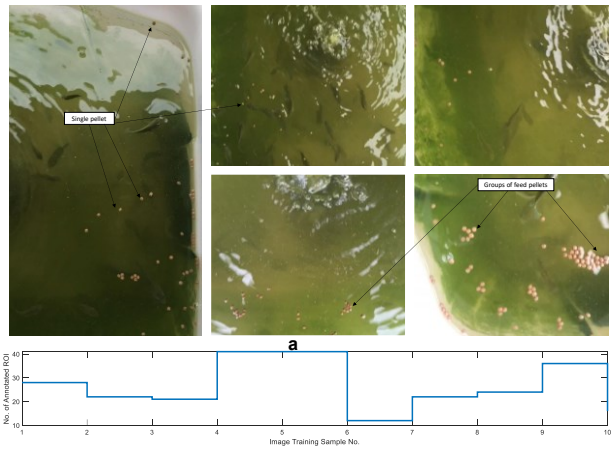

Fig. 2: Sample of images used for training in ACF detector: a) Input images of excess feed on water surface with different background noises, b) No. of annotated ROIs per image

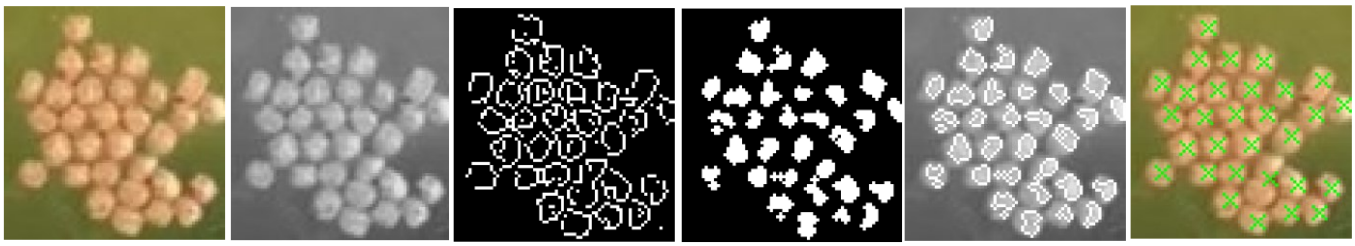

Fig. 3: Workflow of Detection in Each Feed Pellet in a Region Proposal for Group of Feeds

2) Group of Feed Pellets Detection using Sobel Edge Operator

The filtered RP with pixel sizes greater than 20×20, are considered groups of feed pellets wherein the detected region is assumed to contain two or more pellets. To detect and count each pellet in every RP *(see Fig.3)*, the cropped RP in RGB is converted to grayscale before the Sobel edge operator is executed. Specifically, the Sobel operates by convolving two 3×3 masking kernels with the original image, I, to approximate the gradient of the image as depicted in (1) and (2) [23].

$$H_x = \begin{bmatrix} -1 & 0 & 1 \\ -2 & 0 & 2 \\ -1 & 0 & 1 \end{bmatrix} \circledast I \tag{1}$$

$$H_y = \begin{bmatrix} -1 & -2 & -1 \\ 0 & 0 & 0 \\ 1 & 2 & 1 \end{bmatrix} \circledast I \tag{2}$$

It follows that the edges can be calculated by gradient magnitude, GM, in each pixel by (3).

$$GM(x,y) = \sqrt{{H_x}^2 + {H_y}^2} \tag{3}$$

The detected edges from the computation of (3) are then set to a true logical value, while the other pixels were set to logical false to convert the image to binary. To create a blob or fill each detected edge of feeds, a morphological dilation is used such that the binary image A by structuring element B, where $\hat{B}$ reflects B, is operated by (4). The flat morphological structuring element B via `strel` function with the center of the pixel (i,j) was set to a diamond shape with a one-pixel radius. All binary pixel with a true logical value was included in morphological computation describe by (4).

$$A \oplus B = \{z | (\hat{B})_z \cap A^c \neq \emptyset\} \tag{4}$$

After the dilation process, each blob in the binary images was detected as a feed pellet for those with pixel size greater than 10. Each pellet detected in a group of feeds, P_m, was counted. It follows that the overall count of detected pellets, P_t, is the sum of P_m and the count of all single pellets, P_s as depicted in (5). Note that there can be several region proposals for groups of feeds in one image, wherein the total number is denoted by n. The illustrative example of the feed detection in groups is shown in Fig. 3.

$$P_t = P_s + \sum_{i=1}^{n} P_{m_i} \tag{5}$$

D. Evaluation Metrics of the Excess Feed Pellet Counts

The actual count of excess feed pellets, y_i And the estimated count, $\hat{y}_i$, using the ACF detector at different confidence score thresholds and Sobel operator was evaluated with the coefficient of determination (r^2), and normalized root mean square error (NRMSE) as denoted by (7).

$$\text{RMSE} = \sqrt{\sum_{i=1}^{n} \frac{(\hat{y}_i - y_i)^2}{n}} \tag{6}$$

$$\text{NRMSE} = \frac{RMSE}{Y_{max} - Y_{min}} \times 100\% \tag{7}$$

III. Results and Discussions

A. Training Time using ACF Detector

Using the ten training images with 263 annotated feed pellet ROIs, the training time of the ACF detector obtained a mean value of 6.59 seconds for twenty repeated trials, as shown in Fig. 4a. Upon checking the developed ACF detector using 20 testing images, it obtained confidence scores with overall densities peaking around 60 to 100, as shown in Fig. 4b. To remove the RPs with weak confidence scores, only the RPs with certain thresholds were selected. Specifically, at $S > S_s$, wherein $S_s = \{60, 70, 80, 90, 100\}$. Figure 4c shows the detected RPs in every checking image with the corresponding percentage of selected RPs at different confidence score thresholds. As can be seen, the set score thresholds are negatively correlated to the percentage of selected RPs.

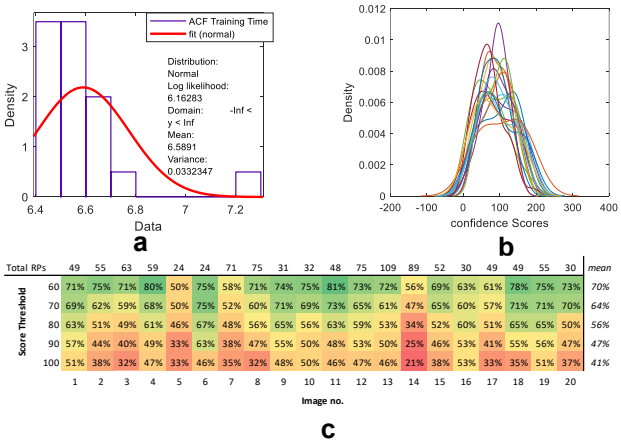

Fig. 4: ACF Training Profile, (a) Training Time of ACF Detector using Input Annotated Images, (b) Confidence Scores of All Region Proposals for Detected Excess Feeds, (c) Heatmap of selected RPs with confidence score thresholds of $S > S_s$ on images for ACF detector testing

B. *Evaluation of the Detected Feed Pellets*

The detected single feed pellets in ACF detector, P_s, and the count of feed pellets in a group, P_m, using Sobel operator are added using equation (5). The output of (5) with different RPs confidence score thresholds was compared to the actual count of feed pellets in every testing image. It follows that the closest feed count estimation is the selected RPs with a confidence score threshold of 60 for both the r^2 and NRMSE, as depicted in Table 1 and Fig. 6. On the other hand, the selected RPs with a confidence score of 100 obtained the lowest performance for both evaluation metrics. As shown in Fig 4c, at $S_s = 60$, there was 70% average selected RPs, or 30% rejected low confidence score RPs. Whereas, at $S_s = 100$, there were only 41% selected RPs. Due to the high rejection of RPs in the latter approach, several undetected feeds with low confidence scores have caused higher estimation discrepancies.

Another factor that contributes to the error in feed counting estimation is when the edges of two or more adjacent feed pellets are connected *(see Fig. 7)*. In this situation, these pellets are detected as one. This challenge is difficult to avoid since the feed pellets are tiny, with an estimated resolution of 20×20 pixels. Also, the radius of the morphological structuring element was set to one pixel—the lowest possible value for morph dilation. In contrast, the higher value of the radius of the structuring element, say 2, will increase the error of counting estimation due to overlapping dilated pixels. To increase the accuracy of the pellet counter, a higher image resolution may be needed, or an enhancement of the images may be used before training.

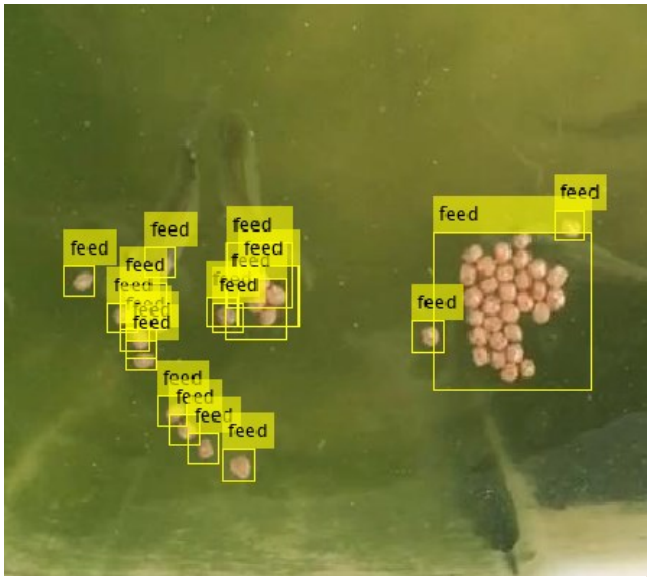

Fig. 5:Example of Detected Feed Pellets with Selected RP Confidence Score >60

IV. Conclusion

Using the ACF and Sobel edge operator, the excess feed pellet counting technique obtained a high correlation between the actual count with *r2* of 0.8 and NRMSE of 11.55% using the confidence score in ACF RPs of greater than 60. The detection of feed pellets' location using the proposed method was effective in different background scenarios such as water reflection, bubbles, random fish, and uneven background color. The training time using the ACF detector was approximately 7 seconds, while the computation time of the excess feed counter after training was around 0.6 seconds. Although the proposed system obtained an acceptable counting accuracy, it can still be improved. Future works include obtaining higher resolution images and image pre-processing to reduce the counting errors caused by the adjacent pellets detected as one.

Table 1: Evaluation Result of Feed Pellet Estimated Count using ACF Detector and Sobel Edge Operator with Different Confidence Scores

Confidence Score Threshold	R^2	NRMSE	Computation Time (s)
60	0.8064	**11.55%**	0.586262
70	0.7308	**16.47%**	0.605626
80	0.6793	**23.96%**	0.538922
90	0.4792	**31.89%**	0.586276
100	0.2319	**40.18%**	0.728284

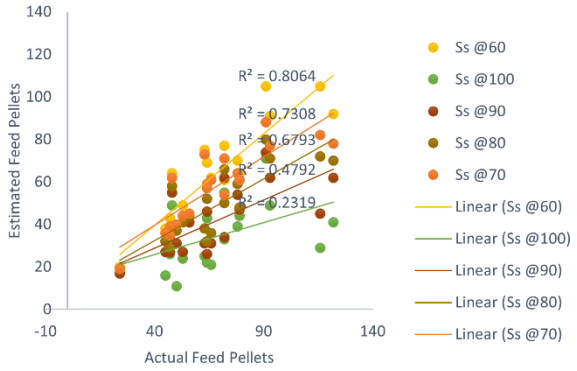

Fig. 6: Scatterplot and Coefficient of Determination for Estimated Count of Feed Pellets and the Actual Count of Feed Pellets

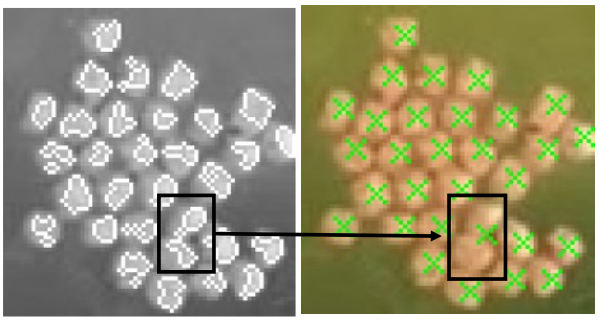

Fig. 7: Error in Feed Pellet Counting (Adjacent Pellets are Detected as One)

Acknowledgment

This research is supported by the Department of Science and Technology (DOST)-Engineering Research and Development for Technology (ERDT), and the Intelligent System Laboratory of De La Salle University.

References

[1] M. P. M. Anvo *et al.*, "Fish meal replacement by Cirina butyrospermi caterpillar's meal in practical diets for Clarias gariepinus fingerlings," *Aquac. Res.*, vol. 48, no. 10, pp. 5243–5250, 2017.

[2] M. Ballester-Moltó, P. Sanchez-Jerez, J. Cerezo-Valverde, and F. Aguado-Giménez, "Particulate waste outflow from fish-farming cages. How much is uneaten feed?," *Mar. Pollut. Bull.*, vol. 119, no.

1, pp. 23–30, 2017.
[3] D. Li, L. Xu, and H. Liu, “Detection of uneaten fish food pellets in underwater images for aquaculture,” *Aquac. Eng.*, vol. 78, no. May, pp. 85–94, 2017.
[4] S. Llorens, I. Pérez-Arjona, E. Soliveres, and V. Espinosa, “Detection and target strength measurements of uneaten feed pellets with a single beam echosounder,” *Aquac. Eng.*, vol. 78, pp. 216–220, 2017.
[5] X. Hu *et al.*, “Real-time detection of uneaten feed pellets in underwater images for aquaculture using an improved YOLO-V4 network,” *Comput. Electron. Agric.*, vol. 185, no. April, p. 106135, 2021.
[6] M. G. B. Palconit *et al.*, “Towards Tracking: Investigation of Genetic Algorithm and LSTM as Fish Trajectory Predictors in Turbid Water,” *IEEE Reg. 10 Annu. Int. Conf. Proceedings/TENCON*, vol. 2020-Novem, no. 1, pp. 744–749, 2020.
[7] R. S. Concepcion, M. G. B. Palconit, E. P. Dadios, J. N. Carpio, R. A. R. Bedruz, and A. A. Bandala, “Arabidopsis Tracker: A Centroid-Based Vegetation Localization Model for Automatic Leaf Canopy Phenotyping in Multiple-Pot Cultivation System,” *2020 IEEE 12th Int. Conf. Humanoid, Nanotechnology, Inf. Technol. Commun. Control. Environ. Manag. HNICEM 2020*, 2020.
[8] L. Yang *et al.*, *Computer Vision Models in Intelligent Aquaculture with Emphasis on Fish Detection and Behavior Analysis: A Review*, no. 0123456789. Springer Netherlands, 2020.
[9] M. G. B. Palconit *et al.*, “Three-Dimensional Stereo Vision Tracking of Multiple Free-Swimming Fish for Low Frame Rate Video,” *J. Adv. Comput. Intell. Intell. Informatics*, vol. 25, no. 5, 2021.
[10] E D. J. Alejandrino, R. Concepcion, V. J. Almero, M. G. Palconit, A. Bandala, “A Hybrid Data Acquisition Model using Artificial Intelligence and IoT Messaging Protocol for Precision Farming,” in *2020 IEEE 12th International Conference on Humanoid, Nanotechnology, Information Technology, Communication and Control, Environment, and Management (HNICEM),* 2020, pp. 1–6.
[11] M. G. B. Palconit and W. A. Nunez, “Statistical analysis of CO2 emission based on road grade, acceleration and vehicle specific power for public utility vehicles: An IoT application,” *IEEE World Forum Internet Things, WF-IoT 2018 - Proc.*, vol. 2018-Janua, pp. 245–250, 2018.
[12] M. G. B. Palconit, A. L. Formentera, R. J. Aying, K. J. A. Dianon, J. B. Tadle, and E. P. Dadios, “Speech Activation for Internet of Things Security System in Public Utility Vehicles and Taxicabs,” *2019 IEEE 11th Int. Conf. Humanoid, Nanotechnology, Inf. Technol. Commun. Control. Environ. Manag. HNICEM 2019*, pp. 1–6, 2019.
[13] M. G. B. Palconit *et al.*, “IoT-Based Precision Irrigation System for Eggplant and Tomato,” *9th Int. Symp. Comput. Intell. Ind. Appl.*, no. November, pp. 0–6, 2020.
[14] M. G. B. Palconit and W. A. Nunez, “Co2 emission monitoring and evaluation of public utility vehicles based on road grade and driving patterns: An Internet of Things application,” *HNICEM 2017 - 9th Int. Conf. Humanoid, Nanotechnology, Inf. Technol. Commun. Control. Environ. Manag.*, vol. 2018-Janua, pp. 1–6, 2017.
[15] R. A. G. Parilla, O. J. C. Leorna, R. D. P. Attos, M. G. B. Palconit, and J. J. A. Obiso, “Low-cost garbage level monitoring system in drainages using internet of things in the Philippines,” *Mindanao J. Sci. Technol.*, vol. 18, no. 1, pp. 164–186, 2020.
[16] U. F. Mustapha, A. W. Alhassan, D. N. Jiang, and G. L. Li, “Sustainable aquaculture development: a review on the roles of cloud computing, internet of things and artificial intelligence (CIA),” *Rev. Aquac.*, 2021.
[17] J. D. Alejandrino *et al.*, “Protocol-Independent Data Acquisition for Precision Farming,” *J. Adv. Comput. Intell. Intell. Informatics*, vol. 25, no. 4, pp. 397–403, 2021.
[18] J. Cao and L. Xu, “Research on Counting Algorithm of Residual Feeds in Aquaculture Based on Machine Vision,” *2018 3rd IEEE Int. Conf. Image, Vis. Comput. ICIVC 2018*, vol. 1, pp. 498–503, 2018.
[19] N. O’Mahony *et al.*, *Deep Learning vs. Traditional Computer Vision BT - Advances in Computer Vision*. Springer International Publishing, 2020.
[20] A. Gupta *et al.*, “Deep Learning in Image Cytometry: A Review,” *Cytom. Part A*, vol. 95, no. 4, pp. 366–380, 2019.
[21] F. A. Hermawati, H. Tjandrasa, and N. Suciati, “Combination of Aggregated Channel Features (ACF) detector and Faster R-CNN to improve object detection performance in fetal ultrasound images,” *Int. J. Intell. Eng. Syst.*, vol. 11, no. 6, pp. 65–74, 2018.
[22] C. Liu, Y. Guo, S. Li, and F. Chang, “ACF based region proposal extraction for YOLOV3 network towards high-performance cyclist detection in high resolution images,” *Sensors (Switzerland)*, vol. 19, no. 12, 2019.
[23] S. Singh, S. Saurav, R. Saini, A. K. Saini, C. Shekhar, and A. Vohra, “Comprehensive Review and Comparative Analysis of Hardware Architectures for Sobel Edge Detector,” *ISRN Electron.*, vol. 2014, pp. 1–9, 2014.
[24] T. S. Kristiansen and A. Fernö, “Individual behaviour and growth of halibut (Hippoglossus hippoglossus L.) fed sinking and floating feed: Evidence of different coping styles,” *Appl. Anim. Behav. Sci.*, vol. 104, no. 3–4, pp. 236–250, 2007.
[25] S. M. Lee and M. A. Pham, “Effects of feeding frequency and feed type on the growth, feed utilization and body composition of juvenile olive flounder, Paralichthys olivaceus,” *Aquac. Res.*, vol. 41, no. 9, pp. 166–171, 2010.
[26] A. M. Abdelhamid, M. F. Salem, and M. El-Sh. Ramadan, “Comparison Between Effects of Sinking and Floating Diets on Growth Performance of the Nile Tilapia (Oreochromis niloticus),” *Egypt. J. Aquat. Biol. Fish.*, vol. 23, no. 2, pp. 347–361, 2019.